International Journal of Modern Physics A
Vol. 36, Nos. 11 & 12 (2021) 2140001 (15 pages)

DOI: 10.1142/S0217751X21400017

Successful application of optical bench in Taiji-1 laser interferometer

Wei Sha[*], Chao Fang[*,§] and Yu Niu[†,‡,¶]

[*]*Changchun Institute of Optics, Fine Mechanics and Physics, CAS, Changchun 130033, China*

[†]*Center for Gravitational Wave Experiment, National Microgravity Laboratory, Institute of Mechanics, Chinese Academy of Sciences (CAS), Beijing 100190, China*

[‡]*Taiji Laboratory for Gravitational Wave Universe (Beijing/Hangzhou), University of Chinese Academy of Sciences (UCAS), Beijing 100049, China*
[§]*fangchao@ciomp.ac.cn*
[¶]*niuyu@imech.ac.cn*

[||]*On behalf of The Taiji Scientific Collaboration*

Received 15 September 2020
Revised 16 October 2020
Accepted 30 October 2020
Published 22 February 2021

As an important part of laser interferometry system, optical bench is one of the core technologies for the detection of spaceborne gravitational waves. As the first step of the space Taiji program, Taiji-1 provides the measurement accuracy of laser interferometry system better than 100 pm/Hz$^{1/2}$(@10 mHz–1 Hz). Taiji-1 is required to be able to track the motion of test mass in inertial sensor. According to the requirements, four interfering optical paths were designed. By adopting an integrated satellite design and selecting the optical and mechanical materials with low linear expansion coefficient, the high stability of optical path was achieved. By using the DOE method, the alignment errors (position/attitude) of four optical paths were all reduced to below 50 μm/100 μrad. In the performance test, the accuracy of laser interferometry system was better than 100 pm/Hz$^{1/2}$(@10 mHz–1 Hz), and the modulation signal of inertial sensor was successfully detected. The results show that all technical indexes of optical bench have met or exceeded the design requirements.

Keywords: Detection of space-borne gravitational wave; laser interferometer; interferometry.

1. Introduction

Gravitational wave astronomy has become a new window for observing the universe. The frequency of gravitational wave signal detected in space is lower than that detected on the ground. The gravitational wave sources in space are more abundant.[1] The principle of gravitational wave detection can be simply described as using laser interferometry to read

[§,¶]Corresponding authors.
[||]For more details, please refer to article 2102002 of this Special Issue.

out the tiny distance change between two reference test masses caused by gravitational wave signal. Therefore, high-precision interferometer is one of the core components of gravitational wave detection system. According to the analysis of Taiji program, the distance variation in an arm length of approximately 3 million kilometers caused by extremely weak gravitational wave is about 10 pm.[2] Therefore, the detection of spaceborne gravitational wave requires a laser interferometry system with high accuracy, that is, the accuracy should be better than 10 pm/Hz$^{1/2}$ in the target measurement frequency band.[3–5] In the Taiji program of Chinese Academy of Sciences, the technical route of laser interferometry system is planned as a three-step route. Taiji-1 experimental satellite is the first step, which aims to verify the key technologies of payloads on orbit. By shortening the arm length of 3×10^6 km into 300 mm, the interferometer system is expected to achieve the measurement accuracy of 100 pm/Hz$^{1/2}$ in the frequency band of 10 mHz–1 Hz. The system is intended to realize the optical readout of the position change of test mass, that is, the real-time measurement of the position change of test mass relative to interferometer.

2. Laser Interferometry System and Payload Configuration

The laser interferometry system consists of a frequency-stabilized laser, acousto-optic frequency shifters, an optical bench and a phase meter. The frequency-stabilized laser emits the laser beam with high frequency stability. Through a pair of acousto-optic frequency shifters, the laser beam is divided into two beams with the relative frequency difference of 1 kHz before entering the optical bench. After being collimated and polarized, the two beams pass through four optical paths in the optical bench to overlap on the QPD. Then the phase information is read out by the phasemeter. Finally, the laser interferometry system evaluates the measurement accuracy by processing the phase information. The system composition is shown in Fig. 1.

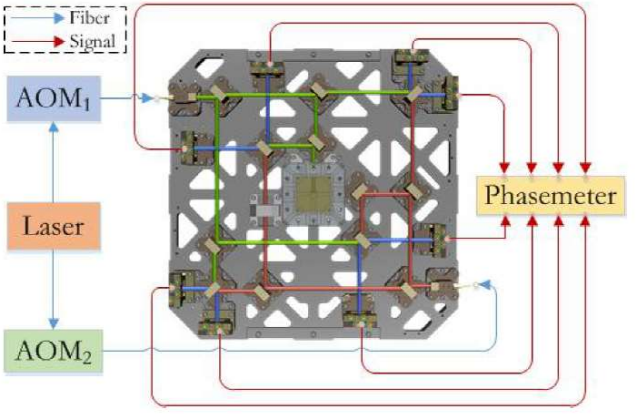

Fig. 1. Composition of laser interferometry system.

Table 1. Time required for the optical path difference fluctuation curve of laser interferometer to become stable under the different temperature amplitudes of heat source.

Composition	Requirement (@10 mHz–1 Hz)
Laser	Frequency stability ≤ 1 MHz/Hz$^{1/2}$
Optical bench	Optical path stability ≤ 60 pm/Hz$^{1/2}$
Phasemeter	Phase readout accuracy ≤ 60 pm/Hz$^{1/2}$

The measurement accuracy of laser interferometry system depends on the frequency stability of laser, the optical path stability of optical bench and the readout accuracy of phase meter. According to the noise model, the accuracy requirements for laser, optical bench and phasemeter are shown in Table 1.

Optical bench is the carrier of the interfering optical path. Its measurement accuracy mainly depends on the stability of optical path. That is, in the process of scientific measurement, the relative positions between optical elements should be kept as stable as possible. In the design and fabrication of optical bench, the main task is to ensure the stability of optical path.

3. Design of Interfering Optical Paths

In order to meet the requirements of scientific tasks, the optical bench is designed with four interfering optical paths, all of which are Mach Zehnder interferometers. Among them, three optical paths are closed loops inside the optical bench, and the rest one is used to read out the motion information of test mass of inertial sensor. The four interfering optical paths are shown in Fig. 2 (FIOS: fiber collimator; BS: bean splitter; PBS: polarization beam splitter; Mir: reflector; RecMir: right-angle reflector; QPD: four quadrant detectors; TM: test mess). The layout of the interfering optical path for measuring the motion of test mass is shown in Fig. 3.

The equal-arm measurement interferometer and the equal-arm reference interferometer are shown in Fig. 4. The two interferometers are symmetrically designed and serve as reference for each other. The interfering optical paths of the two interferometer are both 300 mm. Their function is to suppress the common-mode error sources of the measurement interferometer, such as the vibration of other payloads in satellite and the noise caused by interferometer temperature fluctuation (the expansion and refractive index change of optical elements and fiber).

If there is a gradient in the temperature fluctuation of optical bench, residual temperature noise will still exist after the common-mode suppression. Because the residual noise cannot be reduced, the optical bench must meet very high requirements for temperature uniformity and stability in order to achieve higher measurement accuracy.

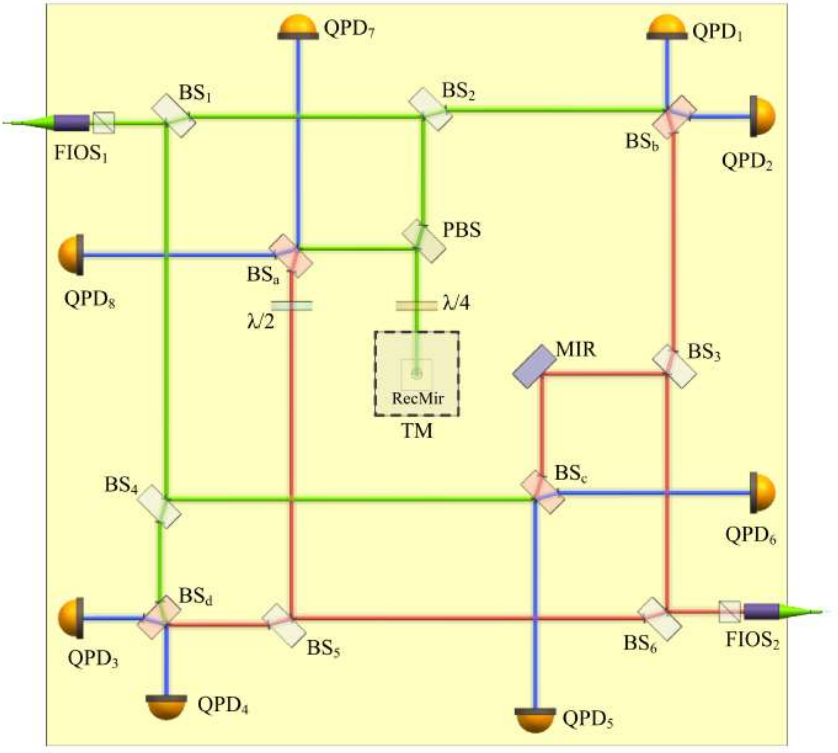

Fig. 2. Composition of laser interferometry system.

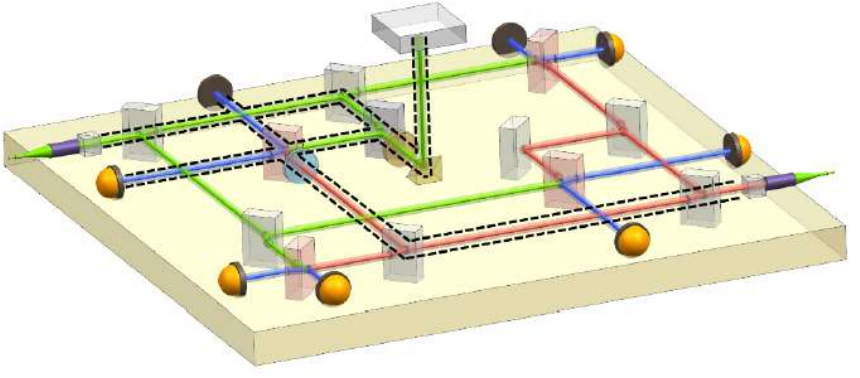

Fig. 3. Composition of laser interferometry system.

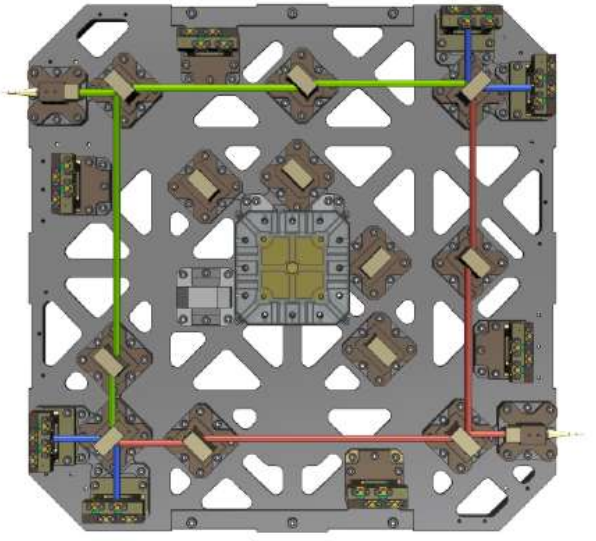

Fig. 4. Design of equal arm interferometer.

Figure 5 shows the laser frequency interferometer, which is an unequal-arm interferometer. The optical path difference between its two interfering beams is constant. As the basis of laser frequency stability and accuracy, this interferometer is mainly used to measure the noise caused by laser frequency fluctuation.

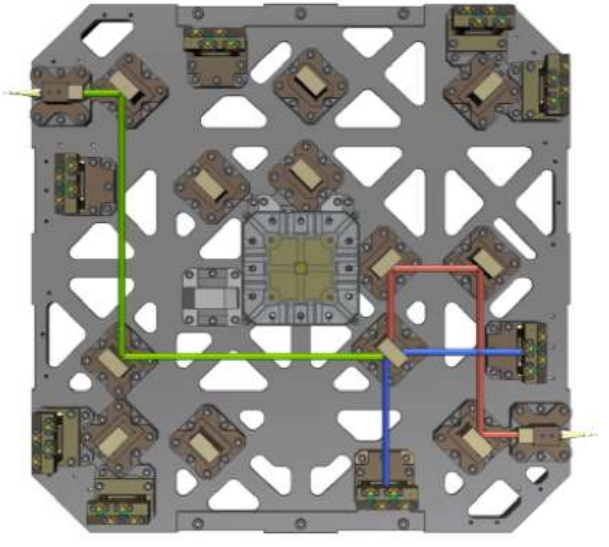

Fig. 5. Design of laser frequency interferometer.

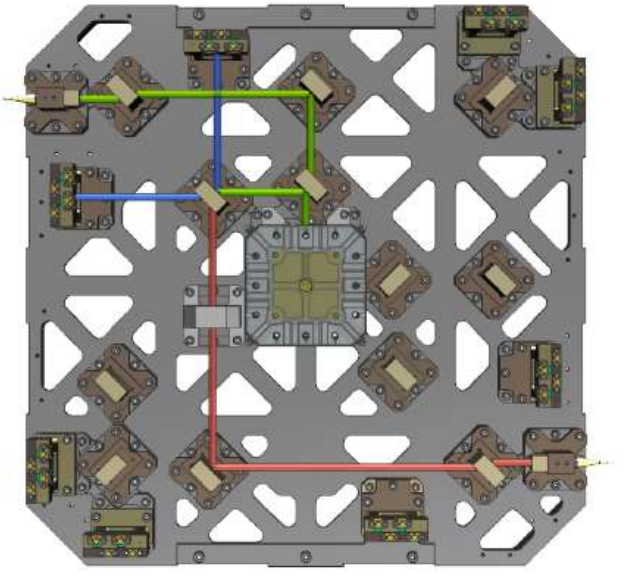

Fig. 6. Design of test mass interferometer.

Figure 6 shows the test mass interferometer. This interferometer is also an unequal-arm interferometer. Because of the movement of test mass, the optical path difference between the two beams is variable. The test mass will move within a very small range ($\leq$ 1 nm) at a very low velocity. Its displacement is within the measurement range of the interferometer.

The test mass interferometer is a three-dimensional optical path, rather than a two-dimensional path. At first, a beam is reflected from a right-angle reflector along the normal direction of the interferometer. After being reflected from the optical surface of test mass, the beam returns along the original path to the interferometer plane through the same right-angle reflector, and then overlaps with another beam.

In the scientific mission, the position change of test mass will be converted into the phase change of interferometer interference signal. After being processed, this displacement will be provided to the satellite as one of the data sources in the free control of satellite drag.

To meet high requirement for measurement accuracy, the opto-mechanical structure should have high stability and environmental adaptability. The major optical elements on optical bench include BS, PBS and wave plate. In order to reduce the deformation and refractive index change of optical elements caused by temperature fluctuation, the fused silica glass with the lowest linear expansion coefficient and stable refractive index has been selected as the substrate of optical elements.

To improve the optical path stability and reduce the temperature stress noise caused by the CTE mismatch between optical material and structural material, invar alloy has

been selected as the structural material of optical bench. In addition, the CTE of invar alloy is strictly limited according to the measured CTE curve of fused silica glass.

4. Design of High-Stability Optical Bench

4.1. *Design of high-stability optical structure*

To meet high requirement for measurement accuracy, the opto-mechanical structure should have high stability and environmental adaptability.

The major optical elements on optical bench include BS, PBS and wave plate. In order to reduce the deformation and refractive index change of optical elements caused by temperature fluctuation, the fused silica glass with the lowest linear expansion coefficient and stable refractive index has been selected as the substrate of optical elements.

To improve the optical path stability and reduce the temperature stress noise caused by the CTE mismatch between optical material and structural material, invar alloy has been selected as the structural material of optical bench. In addition, the CTE of invar alloy is strictly limited according to the measured CTE curve of fused silica glass.

4.2. *Design of high-stability satellite integration*

Apart from the interferometer stability, the on-orbit mechanical and thermal environment fluctuation of the satellite platform will also affect the measurement accuracy. In order to reduce the negative influence of satellite vibration, the method of integration design has been adopted. By using the body-mounted solar panel substrate and the drag-free control system with micro thrusters, the micro-vibration of satellite can be mostly isolated from optical bench. The optical bench needs the highest temperature stability, so it has been placed in the center of the satellite and surrounded by multilayer insulation. Through the combination of active and passive thermal control, the temperature stability of 0.1°C can be achieved.

5. Alignment and Integration of Optical Bench

The amplitude of interference signal is related to the degree of overlap between interfering laser beams. According to the requirement of signal-to-noise ratio, the interference contrast should be more than 70%. According to the decomposition result of alignment accuracy index, the angle between two beams should be smaller than 100 μrad, and the deviation between two spot centroids should be less than 100 μm.[6]

Because of the relatively long length (the longest optical path reaches 520 mm), the optical path is folded several times in order to meet all the requirements in a limited space. Some optical elements are even shared by multiple optical paths. For example, four beam splitters serve two optical paths, each of which couples with at least two other optical paths.

The coupling relation leads to the difficulty in alignment and integration. During the alignment of every optical path, the relative position of each optical element must not exceed the optical tolerance. In addition, because of the dependence of optical paths, the absolute position of each optical element should be finely adjusted according to the design requirement.

In order to satisfy the requirements of beam overlap ratio and relative & absolute position tolerances, the alignment and integration of optical bench is mainly implemented by the following steps:

(1) Analysis of tolerances in optical-element machining and alignment.

By establishing the optical model and using the contrast ratio of interference signal as the objective function, the tolerances were analyzed with the DOE method. The analysis results of optical-element machining are shown in Table 2. In the machining process, the tolerance requirements were enhanced in order to secure a margin large enough. In the implementation process, the machining tolerances of optical elements all met the requirements, as shown in Fig. 7.

Table 2. Time required for the optical path difference fluctuation curve of laser interferometer to become stable under the different temperature amplitudes of heat source.

Optical elements	Requirement		Machining requirement
	Parallelism	Verticality	
PBS	≤ 5”	≤ 5”	≤ 3”
BS	≤ 5”	≤ 5”	≤ 3”
Wave plate	≤ 7”		≤ 5”
Right-angle reflector	45° ± 10”		≤ 7”

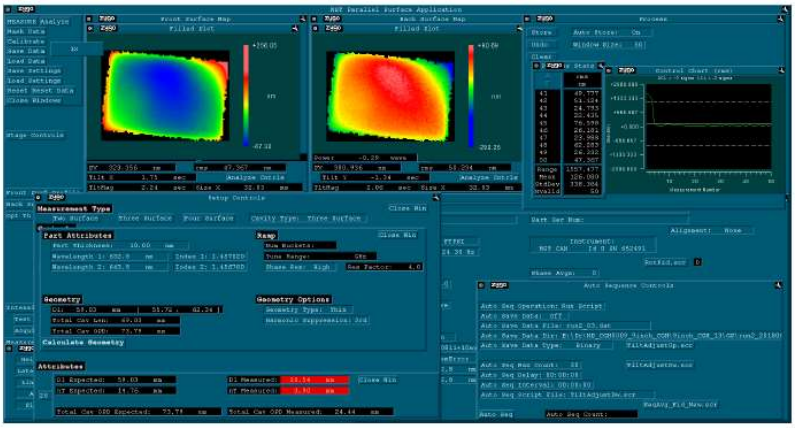

Fig. 7. Design of test mass interferometer.

The misalignment of optical path is reflected in the deviation of absolute and relative positions of optical elements. In the tolerance analysis, the translational and rotational tolerances of main optical elements are taken as parameters, and the weighted global signal contrast ratio is treated as objective. Through the regression analysis of given data sets, the Pareto sensitivity of the parameters is calculated. The evaluation function of global signal contrast ratio is simplified as

$$Y = \sum_{i=1}^{8} |\mathrm{TE}_i| * 10^6 + |\mathrm{TD}_i| * 10^3. \tag{1}$$

The constraints are as follows:

$$\begin{cases} \mathrm{TE}_i \le 100\ \mu\mathrm{rad} \\ \mathrm{TD}_i \le 100\ \mu\mathrm{m} \end{cases}, \tag{2}$$

where TE_i represents the angular deviation of interference beam at the detector i, and TD_i indicates the position deviation of interference beam at the detector i. The magnification in Eq. (1) is to unify the units of angular and position deviations as μrad and μm. The calculation result is shown in Fig. 8. The coupling term of BS1-P (−P and −V, respectively, represent the parallelism and verticality of the corresponding elements) and BSd-P has the greatest impact on global signal contrast ratio and raises it to 5.65%. For example, data fitting is performed for BS1-P and BSd-P to find the coupling relation between the two optical elements. As shown in Fig. 9, the error parameter is used as a factor of the objective function with a nonlinear trend, and is related to other coupling factors. According to the result, the tolerance with high sensitivity needs to be assured in the process of alignment and integration, as shown in Fig. 10.

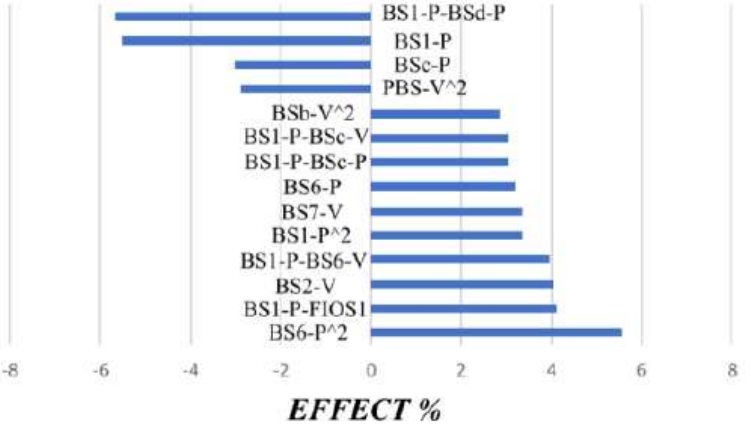

Fig. 8. Sensitivity of major optical elements.

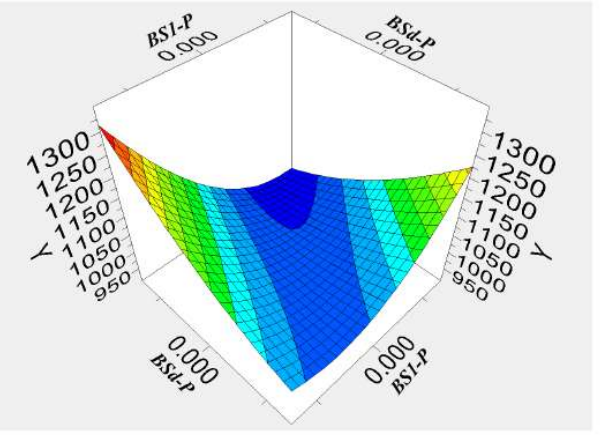

Fig. 9. Coupling relation between two optical elements.

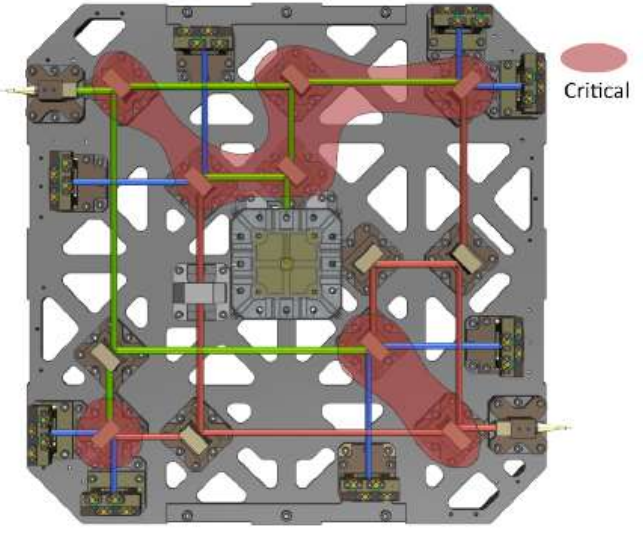

Fig. 10. Optical elements to be assured during alignment and integration.

(2) Establishment of alignment and integration system

The alignment and integration system for the interfering optical paths is composed of a coordinate measuring machine (CMM), a laser beam profiler (LBP), a calibrated quadrant photodiode pair (CQP) and various adjustment tools. CMM and LBP are conventional measurement equipments with the measurement accuracies of 2 μm and

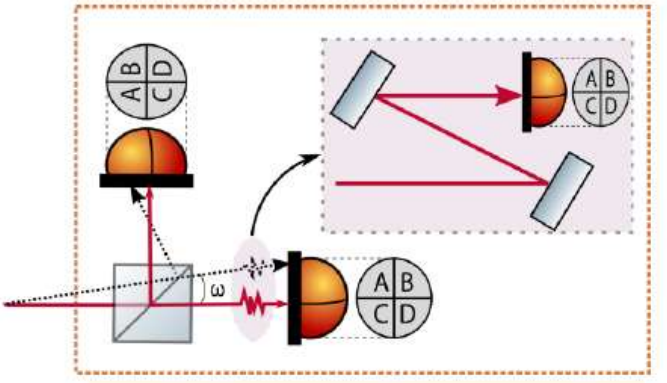

Fig. 11. Concept of CQP.

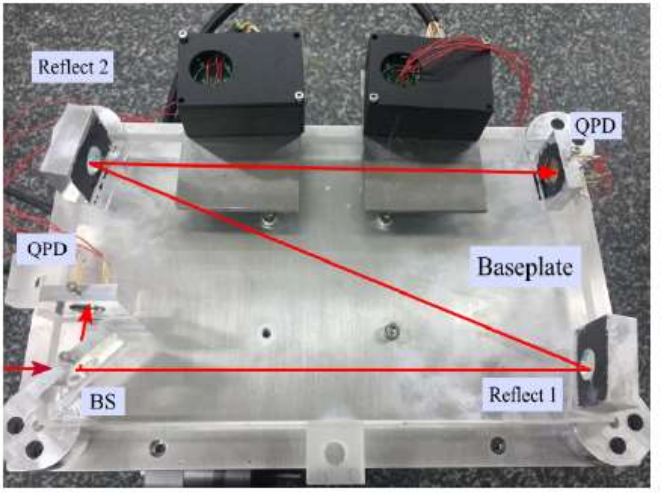

Fig. 12. Photograph of CQP.

1 μm, respectively, which can meet the alignment and integration requirements. CQP is a self-developed measuring device similar to optical lever. Its principle and composition are shown in Figs. 11 and 12, respectively.

(3) Alignment of optical paths

By use of alignment and integration system, the iterative process of optical elements, namely coarse positioning → coarse measurement → fine positioning → fine measurement, can be implemented. During the alignment process, the actual position deviations of optical elements are measured and substituted into the optical model for

Fig. 13. Alignment of equal arm interferometer and laser frequency interferometer.

Fig. 14. Alignment of test mass interferometer.

analysis, in order to investigate their influence on signal contrast ratio and to guide the alignment and integration process.

The alignment status of equal arm interferometer and laser frequency interferometer is shown in Fig. 13. Two sets of CQPs simultaneously monitor the angular deviation and analyze the coupling condition of optical path in real time.[7, 8] The alignment status of test mass interferometer is shown in Fig. 14. The test mass inside the structure is used as a reflector on optical path. The alignment process is confirmed by CQP readout. The measurement of relative position of optical bench by CMM is shown in Fig. 15.

After being adjusted and integrated, the interferometer undergoes the environmental tests and performance tests successively.

The environmental tests of the interferometer mainly include a temperature cycle test, a thermal vacuum test and a mechanical test. The setups of thermal vacuum test, sinusoidal and random vibration test as well as impact test are shown in Figs. 16–18, respectively.

After successfully passing the environmental tests, the laser interferometry system went through the performance test in the Huairou 10-m vacuum test system of the Institute of Mechanics of the Chinese Academy of Sciences. The condition of optical

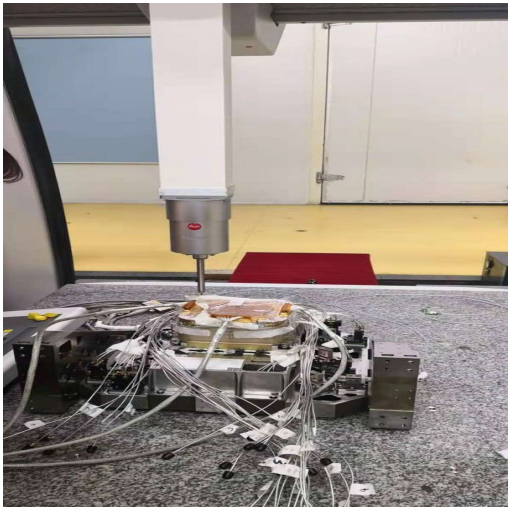

Fig. 15. Relative position measurement by CMM.

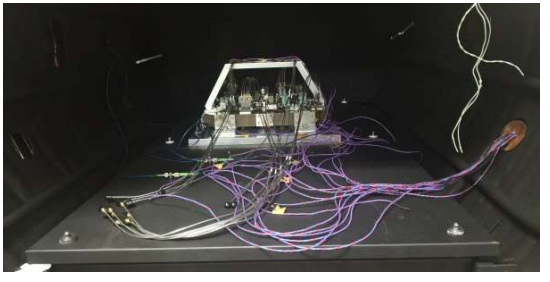

Fig. 16. Thermal vacuum test of optical bench.

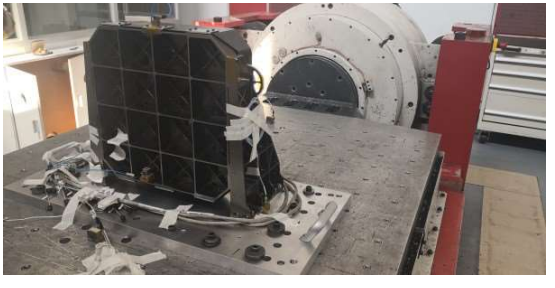

Fig. 17. Sine vibration and random vibration test of optical bench.

Fig. 18. Impact test of optical bench.

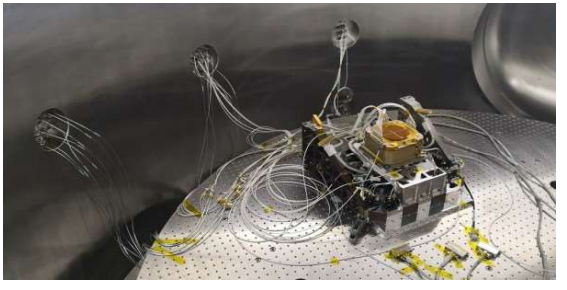

Fig. 19. Performance test of laser interferometry system.

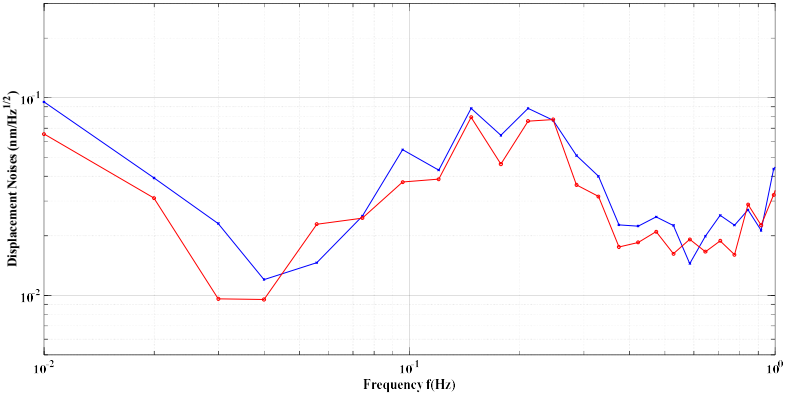

Fig. 20. (Color online) Typical results of Taiji-1 interferometer test on the ground. The results of blue and red lines are tested in different experiments with the same condition.

bench under test in vacuum chamber is shown in Fig. 19. The tests of equal arm interferometer and laser frequency interferometer were completed independently. The test mass interferometer tracked the position change of test mass during the high-voltage suspension test of inertial sensor.

After the processing of test data, the measurement accuracies of the Taiji-1 optical bench were obtained, as shown in Fig. 20. Their measurement accuracies are better than 100 pm/Hz$^{1/2}$@ (10 mHz–1 Hz) and meet the requirement of 100 pm/Hz$^{1/2}$. The test results indicate that the design of laser interferometer system is reasonable, and that all technical indicators of this interferometer meet the design requirements.

In the performance test, thermal control was not put into use, so the actual temperature fluctuation of optical bench was more than 0.1°C. The vibration isolation system could not suppress low-frequency vibration at the frequency of less than 1 Hz. According to the on-orbit thermal analysis, the temperature fluctuation of optical bench will be less than 0.05°C. No component is moving inside the satellite, so there is no vibration source onboard. Therefore, it can be predicted that the on-orbit performance will be better than that on the ground.

6. Conclusion

In the ground performance test, the laser interferometry system of Taiji-1 achieved the measurement accuracy of 100 pm/ Hz$^{1/2}$@ (10 mHz−1 Hz). The test results indicate that the design of laser interferometer system is reasonable. Because of the better environmental condition, more excellent results will be obtained of Taiji-1 in the space. With the accumulated valuable data, it has laid a solid foundation for the building of the upcoming Taiji-2 and Taiji-3.

Acknowledgments

This work was financially supported by the Strategic Priority Research Program of the Chinese Academy of Sciences (Grant Nos. XDA1502070902, XDA1502070304 and XDA1501800003).

References

1. K. Danzmann *et al.*, Albert Einstein insitute hanover, Leibniz University hanover, max planck inst. gravitational phys., Hannover, Germany, Tech. Rep. (2017).
2. W.-R. Hu and Y.-L. Wu, *Natl. Sci. Rev.* **4**, 685 (2017).
3. Z. Luo, S. Bai, X. Bian, G. Chen, P. Dong, Y. Dong, W. Gao, X. Gong, J. He, H. Li *et al.*, *Adv. Mech.* **43**, 415 (2013).
4. Z. Luo, H. Liu and G. Jin, *Opt. Laser Technol.* **105**, 146 (2018).
5. Z. Luo, Z. Guo, G. Jin, Y. Wu and W. Hu, *Results Phys.* **16**, 102918 (2020).
6. Y. Zhao, J. Shen, C. Fang, H. Liu, Z. Wang and Z. Luo, *Opt. Express* **28**, 25545 (2020).
7. Y. Li, H. Liu, Y. Zhao, W. Sha, Z. Wang, Z. Luo and G. Jin, *Appl. Sci.* **9**, 2087 (2019).
8. Y. Li, Y. Zhao, Z. Wang, C. Fang and W. Sha, *IEEE Access* **7**, 112736 (2019).